Indian Journal of Experimental Biology
Vol. 62, March 2024, pp. 206-213
DOI: 10.56042/ijeb.v62i03.3410

Pathogenic potential of biofilm-producing methicillin-resistant *Staphylococcus aureus* in BALB/c mice

Chandrahas Sannat*, SD Hirpurkar, Sanjay Shakya, Nidhi Rawat DK Jolhe, Jasmeet Singh, Tripti Jain, Poornima Gumasta, Anil Patyal, SM Tripathi, MO Kalim, Deepti Kiran Barwa & Shivesh Kumar Deshmukh

Department of Veterinary Microbiology, College of Veterinary Science & Animal Husbandry, Anjora, Durg, Chhattisgarh, India

Received 01 August 2023; *revised 10 October 2023*

Biofilm-forming methicillin-resistant *Staphylococcus aureus* (MRSA) is an emerging pathogen that adversely affects animal and human health. World Health Organization (WHO) has designated MRSA as a high-priority pathogen for research and development. In this study, we have investigated the pathogenic potential of MRSA recovered from mastitic milk of cow. The MRSA was initially characterized for coagulase, haemolytic and DNase activity followed by its biofilm forming ability. Further, an intravenous murine model of MRSA was developed using multiparameter approach comprising of disease activity score, viable bacterial count in blood and tissues; and, detection of biofilm mass in tissue. Infection was successfully established in mice following intravenous inoculation of 3×10^8 colony forming unit (CFU) per mL of MRSA. Fifty percent of MRSA-challenged mice died after infection whereas mice survived exhibited disease activity score >25. Significantly higher MRSA count was recorded in blood, liver and kidney of MRSA-challenged mice as compared to healthy mice (P <0.05). Gram staining revealed the presence of varied size of multiple clusters of Gram-positive biofilm mass in the liver and kidney of MRSA-challenged mice. This study on pathogenesis of MRSA in mice would be useful in not only controlling the MRSA infection, but also in the development of effective therapeutics.

Keywords: Cow milk, Disease activity score (DAS), Mastitic milk, MRSA pathogenesis, Multidrug resistance (MDR)

Multiple drug resistance coupled with ability to form biofilm by methicillin-resistant *Staphylococcus aureus* (MRSA) is an upcoming threat in the control of MRSA infections in animals and humans. Biofilm formation could be accomplished by the expression of fibrinogen and fibronectin-binding proteins along with the co-expression of intercellular adhesion molecules[1,2]. The slow growth rate of bacteria and increased rate of horizontal transfer of resistant genes inside biofilms make the bacteria more tolerant and resistant to antibiotics[3,4]. Methicillin resistance is acquired among *Staphylococcus aureus* by the Staphylococcal cassette chromosome (SCCmec) that encodes a modified penicillin-binding protein having a low affinity towards β-lactam antibiotics[5,6]. Therefore, MRSA tends to develop resistance to many antibiotics including β-lactams, polymyxin, aminoglycosides, cyclic peptides, sulfonamide, quinolone, fluoroquinolone and oxazolidone[7]. According to the World Health Organization (WHO), the MRSA-related public health threat is that 64% people with MRSA infections often die[8].

*Correspondence:
E-Mail: csannat@rediffmail.com

Unlike planktonic form of bacteria, bacterial biofilms induce distinct inflammatory changes in the tissue. Therefore, for characterization of the MRSA-host relationship, understanding the pathology induced by biofilm forming MRSA in the host is necessary. Although, biofilm forming ability of MRSA has been characterized well by several *in vitro* laboratory methods that could not establish the pathogenesis of MRSA in the host. In such cases, an experimental infection in appropriate laboratory animal model would provide a better understanding of the host-bacterium relationship[9]. Virulence factors such as haemolysins, coagulase and polysaccharide intercellular adhesion molecules facilitate initial adhesion and tissue invasion in mammary gland; and thus, biofilm formation by *S. aureus*. Using intravenous mouse model of MRSA, sequential pathology mediated by these virulence determinants in blood stream and disseminated organs such as liver and kidney can be explored. It may aid in identification of appropriate target, and thus the development of effective therapeutic regimens for MRSA infections. Therefore, here, we studied *in vivo* infection in experimental mice model using strong biofilm forming MRSA isolate.

Materials and Methods

Characterization of MRSA isolate

Staphylococcus aureus was isolated from mastitic milk of cow in tryptone soy agar and confirmed through the detection of thermonuclease gene by polymerase chain reaction. It was further characterized up to subspecies (*Staphylococcus aureus* subsp. *aureus*) level by MALDI-TOF mass spectrometry at National Center for Microbial Resources, Pune, India. Methicillin resistance in *Staphylococcus aureus* (MRSA) isolate was detected phenotypically by disc diffusion test using cefoxitin disc (30 µg); and genotypically by PCR using *mecA* gene primer[10].

MRSA isolate (Isolate code SA2018_03) was then characterized for coagulase[11], DNase[12] and haemolytic[13] activity whereas biofilm formation was quantified by microtitre plate test[14]. In microtitre plate test, MRSA isolate was inoculated in 5 mL of tryptone soy broth supplemented with 1% glucose media and incubated at 37ºC for 2-4 h till mid logarithmic phase (0.132 OD_{600nm}). About 100 µL of mid logarithmic culture was then added in eight replicates in well of sterile microtitre plate. One column containing plain media without MRSA served as negative control (NC). The plate was incubated at 37ºC for 24 h with intermittent shaking. Following incubation, contents of each well was poured off and washed with 200 µL of PBS (pH 7.2) for thrice to remove dead and planktonic bacteria. Biofilm forming adherent bacteria were fixed for 10 min with 150 µL of 2% sodium acetate (w/v) and air dried. Each well of microtitre plate was then stained with 150 µL of 0.1% crystal violet (w/v) till 20 min. Excess stain was washed off by washing twice with distilled water. Plate was then air dried and stain was dissolved by treatment with 150 µL of 33% glacial acetic acid (v/v). Biofilm formation was quantified spectrophotometrically in ELISA reader by measuring OD value at 492 nm. Cut off OD value (ODc) was determined as per below mentioned equation:

$$ODc = \text{Average } OD_{NC} + (3 \times \text{standard deviation of } OD_{NC})$$

Intensity of biofilm formation was categorized as given below: Non biofilm former (OD≤ODc); Weak biofilm former (2×ODc≥OD>ODc); Moderate biofilm former (4×ODc≥OD>2×ODc); Strong biofilm former (OD>4×ODc)

Moreover, isolate was screened for biofilm-associated intercellular adhesion genes such as *icaA* and *icaD* (Table 1)[15].

Table 1 — Details of primers and PCR cyclic conditions used for screening of biofilm-associated genes in MRSA

Genes	Primer sequence (5′-3′)	Amplicon size (bp)	PCR cyclic condition
icaA (F)	ACACTTGCTGGCGCAGTCAA	188	35 cycles of denaturation (94°C for 30 s), annealing (58°C for 30 s), and extn (72°C for 30 s)
icaA (R)	TCTGGAACCAACATCCAACA		
icaD (F)	ATGGTCAAGCCCAGACAGAG	198	
icaD (R)	AGTATTTTCAATGTTTA AAGCAA		

Experimental animals

The current study used female BALB/c mice (n=12; 25±3 g). The experiment was approved by the ethical committee of Veterinary College, Anjora, Durg, Chhattisgarh, India.

Preparation of MRSA infection stock

Five MRSA colonies grown on tryptone soy agar were diluted in 5 mL of tryptone soy broth to form a uniform suspension and incubated at 37°C for 4 h. Following centrifugation (1500 rpm for 10 min) of broth culture, bacterial cell pellet was obtained. Bacterial cell pellet was washed four times with PBS (pH 7.2) and then diluted in PBS (pH 7.2) to the desired concentration (3×10^8 CFU/mL) after determining actual colony forming unit (CFU) using standard plate count method[16].

Whole blood survival assay

About 25 µL of MRSA suspension (3×10^8 CFU mL^{-1}) was mixed in triplicate with 75 µL of fresh murine heparinized blood in a microtitre plate and incubated at 37°C. Ten µL of MRSA culture was taken from each well at 0, 1, 3, 5 and 24 h and plated on Luria Bertani agar. The number of colonies on each plate was counted after 24 h of incubation at 37°C. The colony-forming unit (CFU) per milliliter of blood was calculated as follows:

$$(\text{CFU mL}^{-1}) = \frac{\text{Average numbers of colony}}{\text{Inoculum size of the sample}} \text{ X dilution factor}$$

MRSA infection in mice

The experimental model consisted of two groups of BALB/c mice: infection (n=6) and control (n=6). Mice were anaesthetized by an intramuscular dose of ketamine hydrochloride @ 87.5 mg kg^{-1} body wt.) and xylazine @13 mg kg^{-1} body wt. The mice in the control group received normal saline (100 µL), whereas the mice in the infection group were given MRSA (3×10^7 CFU in 100 µL) via slow intravenous infusion in the tail vein. Mice were observed daily for 8 days and any deviation from optimal body parameters (mortality, body weight, appearance of eye and fur, posture and motility) was recorded.

Disease activity score (DAS)

Each mouse's disease activity score (DAS) was determined using the body scoring system with little modification (Table 2)[17], and animals were categorized as follows: Healthy (≤50; Mild sick (10≥DAS>5); Moderately sick (25≥DAS>10); Severely sick (35≥DAS>25); and Moribund (DAS>35).

Viable bacterial load in blood and tissues

The blood sample was taken before infection, as well as at 48, 96 and 120 h post-infection (PI).The mice that died during the experiment were subjected to the post-mortem examination, and; the mice that survived were sacrificed on day-8 PI. Pieces of kidney and liver tissue were collected aseptically from dead/sacrificed mice in both sterile PBS (pH 7.2) and 10% formalin. MRSA was recovered from blood, liver, and kidney using bacterial culture and PCR. Viable bacterial load in the kidney, liver and blood was determined separately by the standard plate count method[16].

Virulence characterization of recovered MRSA isolates

MRSA isolates recovered from blood and tissues of infected mice were characterized further for coagulase[11], DNase[12], haemolytic[13] activity and biofilm formation by microtitre plate test[14].

Histopathology

Histopathology of kidney and liver tissue collected in 10% formalin was done by hematoxylin and eosin (H & E) staining[18].

Table 2 — Scoring of body parameters of mice to determine disease activity score (DAS)

Parameters	Score	Cumulative score
Bodyweight		
No change	0	25
Loss of body wt. <25% (1% loss= 1 point)	1-24	
Loss of body wt. >25%	25	
Fur		
Shining	0	15
Matte	10	
Ruffled	15	
Eyes		
Clear/clean	0	10
Unclean and sticky	5	
Semiclosed/closed	10	
Posture		
Normal	0	25
Hunched	15	
Massively hunched	25	
Motility		
Spontaneous	0	
Moderately reduced activity	5	25
Motility after stimulation	15	
Isolation, lethargy, coordination disorders	25	
		100

Gram staining of tissue

After clearing the tissue in xylene, sequential passage was done in 100, 80 and 50% alcohol. Then slides were kept in a primary stain solution of crystal violet for 5 min which was followed by twice washing in tap water, fixing in Gram's iodine for 2 min, decolourization with 70% ethanol for 30 s followed by quick rinsing in water. Finally, tissue sections were kept in safranin solution for 2 min. It was then dehydrated in a series of alcohols (50, 80 and 100%), cleared in xylene, and then covered with cover slip. Gram-positive spots were counted microscopically per 50 high power (40X) fields using T capture micrometry software and approximate size (in μm) was measured.

Statistical analysis

Generated data were analyzed by SPSS computer software and; mean values, standard error and p-values were recorded. Data having p-values<0.05 were designated significant.

Results and Discussion

Virulence markers in MRSA isolate

MRSA isolate was coagulase and DNase positive and; showed β-hemolysis. Isolate was detected strong biofilm former (3.24 Mean OD_{492nm}) and harboured *icaA* as well as *icaD* gene. Coagulase contributes to chronicity of infection and unresponsiveness towards the conventional antibiotic treatment because coagulase generate a fibrin shield in abscess which protect microorganism from immune cell infiltration and/or antibiotics thereby promote bacterial survival and dissemination in tissue[19,20]. DNase aggravates the infection through the degradation of neutrophil extracellular traps that cause the escape of bacteria from the phagocytic action of neutrophils[21]. β-hemolysin is important for infectious colonization and help the organism evade from immune mechanism[22,23]. Biofilm-forming ability of MRSA is because of slime production which is further influenced by the expression of intercellular adhesion genes[24]. By and large, co-expression of *icaA* and *icaD* increases *N*-acetyl glucosaminyl transferase activity, polysaccharide intercellular adhesion protein (PIA) synthesis, and thus slime production[2,25].

Growth kinetic of MRSA in murine blood

The MRSA isolate survived, got adapted, and then grew successfully in murine blood. After an initial drop in bacterial load in blood at 1 h post-incubation, progressive increase was recorded up to 24 h of

incubation at 37ºC (Fig. 1) as reported by Kwiecinski *et al*.[26]. Intravenous murine model was therefore selected for study of MRSA infection in mice.

Establishment of MRSA infection in mice

Following intravenous inoculation of 3×10^8 CFU mL^{-1} of MRSA in BALB/c mice, organisms are disseminated into tissue, and form abscesses. The establishment of clinical disease in mice could be attributed to the effect of growth phases on expression of virulence factors in MRSA[27,28]. For instance, colonization factors are expressed during logarithmic phase while effectors in the stationary phase[29].

Mortality of MRSA-challenged mice

In the infected group, three out of six mice (50%) succumbed to MRSA infection. One mouse died at 20 h after infection, second at 40 and the third mice at 42 h PI. Mortality of MRSA-infected mice could be associated with a wide array of virulence determinants associated with MRSA including haemolysins, coagulase, DNase and determinants of biofilm formation[27,30,31].

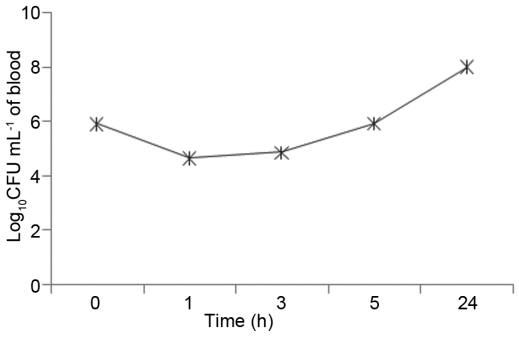

Fig. 1 — Growth kinetics of MRSA organism in murine blood at incubation temperature of 37ºC at various point of time post incubation

Effect on various body parameters and disease activity score (DAS)

Mice in the healthy control group gained weight gradually, whereas infected mice lost weight at a rate ranging from 4.42 to 7.85% over eight days (Fig. 2). On days 1 and 2, a significant reduction in body weight was observed (P <0.05), followed by a steady reduction up to day 5, and then a constant body weight was recorded. Body parameter scores in the current study were more (P <0.05) in the mice challenged with MRSA than in that of healthy group of mice (Table 3). Mice from the control group remained healthy (DAS <5) throughout the

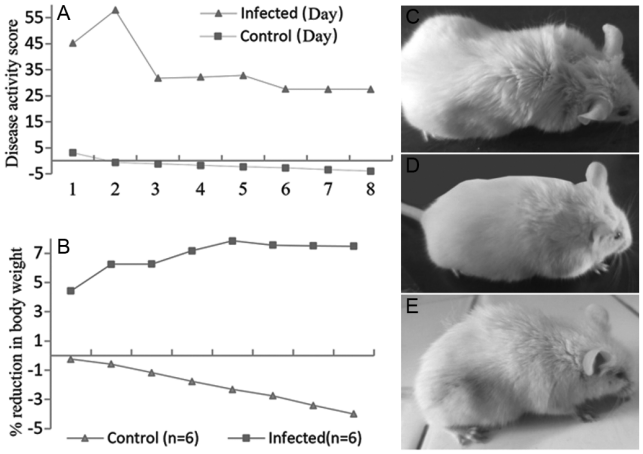

Fig. 2 — Assessment of disease progression in MRSA-challenged BALB/c mice (A & B) Disease activity score; and Percent reduction in body weight of mice at day-1 to day-8 post infection; (C) Ruffled fur at 18 h post infection; and (D & E) Hunched posture in mice at 20 & 40 h post infection

Table 3 — Disease activity score of mice after MRSA infection

Body Parameters	Group	Body parameter score							
		Day 1	Day 2	Day 3	Day 4	Day 5	Day 6	Day 7	Day 8
Bodyweight	Infected	4.42±1.18^a	6.26±1.08^a	6.27±1.79^a	7.18±2.41^a	7.85±3.08^a	7.56±3.22^a	7.51±4.05^a	7.49±4.26^a
	Control	–0.24±0.31^b	–0.58±0.44^b	–1.16±0.51^b	–1.76±0.62^b	–2.32±0.60^b	–2.75±0.57^b	–3.42±0.75^b	–3.99±0.79^b
Fur	Infected	10.00±2.24^a	10.00±2.74^a	8.33±4.41^a	8.33±4.41^a	8.33±4.41^a	6.67±3.33^a	6.67±3.33^a	6.67±3.33^a
	Control	1.67±0.27^b	0.00±0.00^b	0.00±0.00^b	0.00±0.00^b	0.00±0.00^b	0.00±0.00^b	0.00±0.00^b	0.00±0.00^b
Eyes	Infected	5.83±0.83^a	6.00±1.87^a	5.00±0.00^a	5.00±0.00^a	5.00±0.00^a	1.67±1.67^a	1.67±1.67^a	1.67±1.67^a
	Control	0.00±0.00^b	0.00±0.00^b	0.00±0.00^b	0.00±0.00^b	0.00±0.00^b	0.00±0.00^b	0.00±0.00^b	0.00±0.00^b
Posture	Infected	11.67±4.01^a	14.00±4.01^a	10.00±5.00^a	10.00±5.00^a	10.00±5.00^a	10.00±5.00^a	10.00±5.00^a	10.00±5.00^a
	Control	0.00±0.00^b	0.00±0.00^b	0.00±0.00^b	0.00±0.00^b	0.00±0.00^b	0.00±0.00^b	0.00±0.00^b	0.00±0.00^b
Motility	Infected	13.33±4.01^a	21.67±4.90^a	1.67±1.67^a	1.67±1.67^a	1.67±1.67^a	1.67±1.67^a	1.67±1.67^a	1.67±1.67^a
	Control	1.67±0.27^b	0.00±0.00^b	0.00±0.00^b	0.00±0.00^b	0.00±0.00^b	0.00±0.00^b	0.00±0.00^b	0.00±0.00^b
DAS	Infected	45.25	57.93	31.78	32.18	32.85	27.57	27.52	27.5
	Control	3.09	–0.58	–1.16	–1.76	–2.32	–2.75	–3.42	–3.99
Level of sickness	Infected	Moribund	Moribund	Severe sickness	Severe sickness	Severe sickness	Severe sickness	Severe sickness	Severe sickness
	Control	Animals healthy	Animals healthy	Animals healthy	Animals healthy	Animals healthy	Animals healthy	Animals healthy	Animals healthy

[Mean values with different superscripts in the columns for particular body parameter scores differ significantly (P <0.05)]

experiment whereas MRSA infected mice showed DAS >25 (Table 3 and Fig. 2). MRSA infected mice exhibited ruffled and matted fur, sticky eyes, hunched posture and reduced motility.

Initial weight loss in mice following MRSA infection could be due to initial bacteremia, inflammatory response, and sepsis, all of which led to a decrease in food intake[32,33]. Bodyweight recovery following day 5 PI was accompanied by decreased bacteremia, as evidenced by a decrease in bacterial load in blood on day 5 PI.

The DAS is comprised of a wide range of measures that reflect the severity of infection. The mice in the control group remained healthy throughout the study period (DAS <5). During the 8-day study period, each of the mice in the MRSA-infected group developed symptoms and showed DAS >25. Higher DAS (>35) on day-1 and day-2 PI could be attributed to the moribund status of 50% of mice during the first two days of PI. MRSA-induced inflammation, bacteremia, and sepsis all contributed to an overall worsening of mice's condition[33]. Following that, similar levels of sickness were observed in mice, indicating recovery from infection.

Bacterial load in blood, kidney and liver

The MRSA organism was re-isolated from the blood, liver and kidney of the mice post infection and tested positive by PCR using *nuc* gene primer. A significantly higher bacterial count (P <0.05) was recorded in the blood of the infected mice at 48 h PI with further reductions at 96 and 120 h. Infected mice had a significantly higher bacterial load (P <0.05) in the kidneys than in the liver (Fig. 3).

The gradual decrease in bacterial load over time is attributed to dissemination of MRSA organisms from the bloodstream to vascular organs following bacteremia. The recovery of MRSA from kidney and liver tissue demonstrated the spread of infection to the liver and kidneys via systemic circulation and thus could be considered as organs primarily affected by MRSA after intravenous inoculation in mice[33-35]. The higher bacterial load in the kidney compared to the liver is consistent with the earlier findings[36,37]. During the bacteremic stage, macrophages and neutrophils are the important blood cells that enable the spread of bacteria to other organs[3].

Virulence determinants of MRSA organism re-isolated from MRSA-infected mice

MRSA isolates recovered from blood, liver and kidney of MRSA-challenged mice retained the virulence property of MRSA organism. Recovered isolates were positive for coagulase and DNase; and showed beta haemolysis on 5% calf blood agar. Each of the recovered MRSA isolates was adjudged as strong biofilm former by microtitre plate test.

Gram-positive spots in kidney and liver

Gram staining revealed the presence of multiple clusters of Gram-positive spots or biofilm mass ranging in size from 5 to 50 µm in the liver and kidney of MRSA infected mice (Fig. 3). The extent of

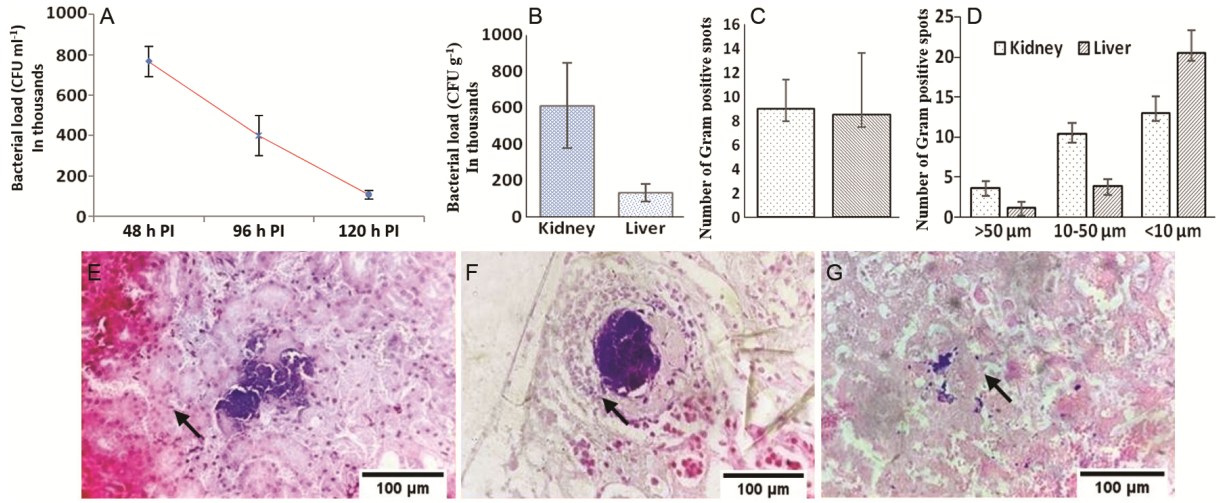

Fig. 3 — Bacterial density and Gram positive spots in tissues of MRSA-challenged mice. Mean bacterial load (A) in blood collected from mice at various point of time post infection; and (B) in tissues of sacrificed and dead mice; (C & D) Number of Gram positive spots per 50 high power field; and (D) Relative size of Gram positive spots in liver and kidney of infected mice; (E) Macro cluster containing several large Gram-positive spots in the kidney at 40 h PI; (F) Large Gram-positive spots in the kidney at 20 h PI; and (G) Small and moderate size Gram-positive spots in liver at 40 h PI (Gram staining 400X)

MRSA biofilm formation can be interpreted indirectly by the formation of Gram-positive spots, which are influenced by bacterial density in tissue. Gram-positive aggregates seen in the kidney and liver are therefore most likely representing MRSA *in vivo* biofilm[38]. Small-sized Gram-positive spots (<10 µm) were predominant. The size of the Gram-positive spots in the liver and kidney varied significantly (P <0.05) but not the number of Gram- positive spots. Large-sized Gram-positive spots ranging in width from 53- 97 µm and length from 90-216 µm were discovered in the kidney (Fig. 3). Relatively smaller spots of 20-29 µm wide and 40-53 µm in long were recorded in the liver. The kidney showed macro clusters with several large Gram-positive spots whereas the liver displayed large numbers of small-sized Gram-positive spots. Large Gram-positive spots in the kidney could be due to higher bacterial load in kidney than in the liver. MRSA organisms tend to produce slime which mediates strong adherence of organisms in clusters to form a biofilm followed by encapsulation of bacterial nidus with fibrin deposits[2,20]. Protection of bacteria from adverse host environments by biofilms causes an added complication in antimicrobial resistance. Quantifying and determining the biofilm biomass in the tissue could be employed in *in vivo* assessment of antibiofilm activity of an agent.

Gross and histomorphology of kidney and liver

Mice in the control group had normal liver and kidney architecture. The kidney in the MRSA-infected group had multiple abscesses, and the liver had necrotic foci, hemorrhages and gross congestion (Fig. 4). On histopathology microabscess, degeneration and necrosis were the predominant findings in kidneys, followed by hemorrhages and glomerular atrophy whereas hepatic lesions included degeneration and necrosis, infiltration of mononuclear cells, and congestion[39]. Extensive inflammatory changes in liver and kidney could be attributed to combined effect of haemolysins, DNase, coagulase and biofilm forming ability of MRSA organisms. Enhanced adherence of MRSA organisms to epithelial cells by α- and β- toxins[22,23], degradation of extracellular DNA in neutrophil extracellular traps by DNase and formation of a fibrin capsule by coagulase lead to encapsulation of organisms which facilitates survival of bacteria and tissue destruction, resulting in abscess maturation at organ surfaces[19,21,40]. Strong biofilm forming ability of MRSA could be due to concomitant presence of both the intercellular adhesion genes (*icaA* and *icaD*) responsible for slime production in biofilm matrix[2,25]. Finally, liquefaction necrosis and organism dissemination occur in new sites, leading to the formation of multiple lesions[20,41].

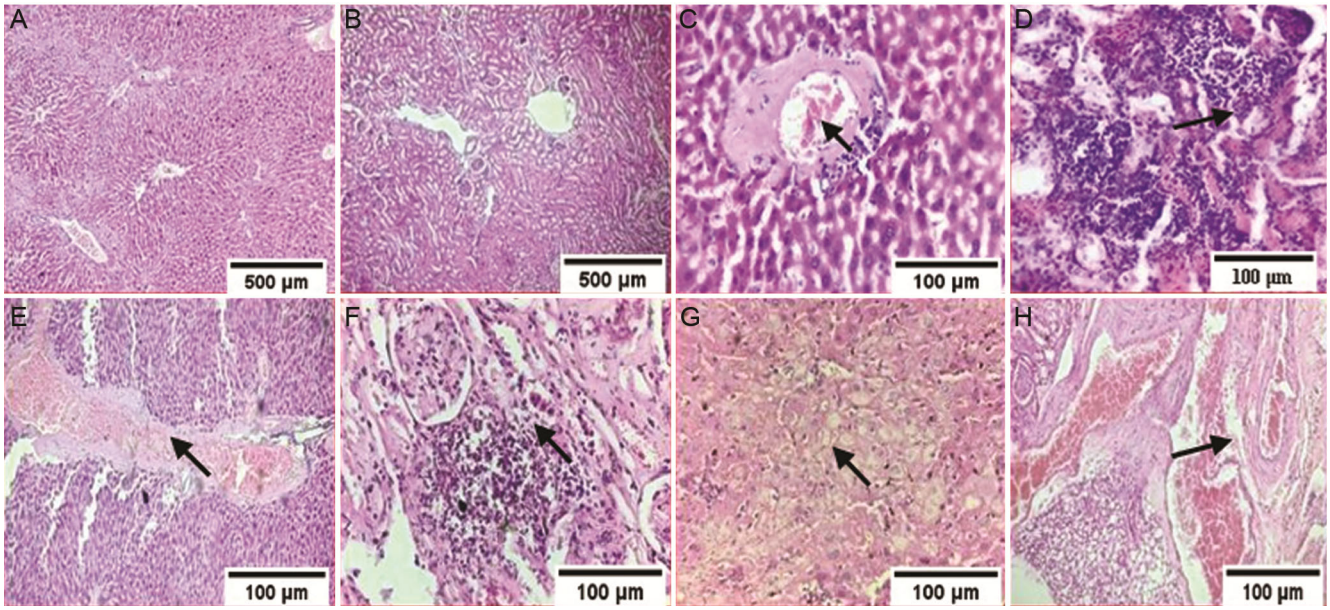

Fig. 4 — Sequential pathology of liver and kidney from MRSA-challenged BALB/c mice. Normal architecture of (A) Liver; (B) Kidney; (C) Mononuclear cell infiltration in liver at 40 h post infection; (D) Severe congestion in central vein of liver at day-8 post infection; (E) Coagulative necrosis in liver at day-8 post infection; (F) microabscess in kidney at 40 h post infection; (G) Degeneration and necrotic foci in kidney at 20 h post infection; and (H) Severe congestion in kidney at day-8 post infection. (H &E 400X)

Conclusion

Current intravenous murine model was reproducible and robust experimental system for *in vivo* investigations conducted for methicillin-resistant *Staphylococcus aureus* (MRSA) infection in mice. Establishment of bacteremia and sepsis in BALB/c mice were done through glut of virulence markers viz. coagulase, DNase, haemolysin and biofilm forming ability. Present investigation emphasizes the use of simple and economical method of Gram staining for quantifying the biofilm biomass in host tissues. The results suggest a multiparameter approach for investigation of MRSA infection in BALB/c mice for identification of appropriate targets to develop anti-MRSA strategy. Biofilm forming ability of MRSA enhances the pathogenicity of organism and could be the possible cause of intolerance of MRSA towards antibiotics. In this context, the current study emphasizes development and use of antimicrobials in combination with antibiofilm agent to overcome antibiotic tolerance arising due to biofilm.

Conflict of interest

Authors declare no competing interests.

References

1 François P, Schrenzel J & Götz F, Biology and Regulation of Staphylococcal Biofilm. *Int J Mol Sci*, 24 (2023) 5218.

2 Pidwill GR, Gibson JF, Cole J, Renshaw SA & Foster SJ, The Role of Macrophages in *Staphylococcus aureus* Infection. *Front Immunol*, 19 (2021) 620339.

3 Rather MA, Gupta K & Mandal M, Microbial biofilm: formation, architecture, antibiotic resistance, and control strategies. *Braz J Microbiol*, 52 (2021)1701.

4 Shree P, Singh CK, Sodhi KK, Surya JN & Singh DK, Biofilms: understanding the structure and contribution towards bacterial resistance in antibiotics. *Med Microecol*, 16 (2023) 100084.

5 Fergestad ME, Stamsås GA, Morales Angeles D, Salehian Z, Wasteson Y & Kjos M, Penicillin-binding protein PBP2a provides variable levels of protection toward different β-lactams in Staphylococcus aureus RN4220. *Microbiology Open*, 9 (2020) e1057.

6 Zhu Z, Hu Z, Li S, Fang R, Ono HK & Hu D-L, Molecular Characteristics and Pathogenicity of *Staphylococcus aureus* Exotoxins. *Int J Mol Sci*, 25 (2024) 395.

7 Yehia HM, Al-Masoud AH, Alarjani KM & Alamri MS, Prevalence of methicillin-resistant (*mecA*gene) and heat-resistant *Staphylococcus aureus* strains in pasteurized camel milk. *J Dairy Sci*, 103 (2020) 5947.

8 Nandhini P, Kumar P, Mickymaray S, Alothaim AS, Somasundaram J & Rajan M, Recent Developments in Methicillin-Resistant *Staphylococcus aureus* (MRSA) Treatment: A Review. *Antibiotics* (Basel), 11 (2022) 606.

9 Howden BP, Giulieri SG, Wong Fok Lung T, Baines SL, Sharkey LK, Lee JY, Hachani A, Monk IR & Stinear TP, *Staphylococcus aureus* host interactions and adaptation. *Nat Rev Microbiol*, 27 (2023) 1.

10 Abdelwahab MA, Amer WH, Elsharawy D, Elkolaly RM, Helal RAEF, El Malla DA, Elfeky YG, Bedair HA, Amer RS, Abd-Elmonsef ME & Taha MS, Phenotypic and Genotypic Characterization of Methicillin Resistance in *Staphylococci* Isolated from an Egyptian University Hospital. *Pathogens*, 12 (2023) 556.

11 Aqel H, Sannan N & Foudah R, From Hospital to Community: Exploring Antibiotic Resistance and Genes Associated with Virulence Factor Diversity of Coagulase-Positive *Staphylococci*. *Antibiotics* (Basel), 12 (2023) 1147.

12 Canning B, Mohamed I, Wickramasinghe N, Swindells J & O'Shea MK, Thermonuclease test accuracy is preserved in methicillin-resistant *Staphylococcus aureus* isolates. *J Med Microbiol*, 69 (2020) 548.

13 Liu Y, Shi Y, Cheng H, Chen J, Wang Z, Meng Q, Tang Y, Yu Z, Zheng J & Shang Y, Lapatinib Acts against Biofilm Formation and the Hemolytic Activity of *Staphylococcus aureus*. *ACS Omega*, 7 (2022) 9004.

14 Basnet A, Tamang B, Shrestha MR, Shrestha LB, Rai JR, Maharjan R, Dahal S, Shrestha P & Rai SK, Assessment of four in vitro phenotypic biofilm detection methods in relation to antimicrobial resistance in aerobic clinical bacterial isolates. *PLoS One*, 18 (2023) e0294646.

15 Abdel-Shafi S, El-Serwy H, El-Zawahry Y, Zaki M, Sitohy B & Sitohy M, The Association between *icaA* and *icaB* Genes, Antibiotic Resistance and Biofilm Formation in Clinical Isolates of Staphylococci spp. *Antibiotics* (Basel), 11 (2022) 389.

16 Jiang H, Wang K, Yan M, Ye Q, Lin X, Chen L, Ye Y, Zhang L, Liu J & Huang T, Pathogenic and Virulence Factor Detection on Viable but Non-culturable Methicillin-Resistant *Staphylococcus aureus*. *Front Microbiol*, 12 (2021) 630053.

17 Trübe P, Hertlein T, Mrochen DM, Schulz D, Jorde I, Krause B, Zeun J, Fischer S, Wolf SA, Walthe B, Semmler T, Bröker BM, Ulrich RG, Ohlsen K & Holtfreter S, Bringing together what belongs together: Optimizing murine infection models by using mouse-adapted *Staphylococcus aureus* strains. *Int J Med Microbiol*, 309 (2019) 26.

18 Suvarna SK, Layton C & Bancroft JD, Bancroft's Theory & practice of histological technique (Elsevier Limited) 2019, 114.

19 Nappi F & Avtaar Singh SS, Host–Bacterium Interaction Mechanisms in *Staphylococcus aureus* Endocarditis: A Systematic Review. *Int J Mol Sci*, 24 (2023) 11068.

20 Wójcik-Bojek U, Różalska B & Sadowska B, *Staphylococcus aureus*—A Known Opponent against Host Defense Mechanisms and Vaccine Development—Do We Still Have a Chance to Win?. *Int J Mol Sci*, 23 (2022) 948.

21 Singh J, Boettcher M, Dölling M, Heuer A, Hohberger B, Leppkes M, Naschberger E, Schapher M, Schauer C, Schoen J, Stürzl M, Vitkov L, Wang H, Zlatar L, Schett GA, Pisetsky DS, Liu ML, Herrmann M & Knopf J, Moonlighting chromatin: when DNA escapes nuclear control. *Cell Death Differ*, 30 (2023) 861.

22 Gordon YCC, Justin SB & Michael O, Pathogenicity and virulence of *Staphylococcus aureus*. *Virulence*, 12 (2021) 547.

23 Campos B, Pickering AC, Rocha LS, Aguilar AP, Fabres-Klein MH, de Oliveira Mendes TA, Fitzgerald JR & de

Oliveira Barros Ribon A, Diversity and pathogenesis of *Staphylococcus aureus* from bovine mastitis: current understanding and future perspectives. *BMC Vet Res*, 18 (2022) 115.

24 Silva V, Almeida L, Gaio V, Cerca N, Manageiro V, Caniça M, Capelo JL, Igrejas G & Poeta P, Biofilm Formation of Multidrug-Resistant MRSA Strains Isolated from Different Types of Human Infections. *Pathogens*, 10 (2021) 970.

25 Nguyen HTT, Nguyen TH & Otto M, The staphylococcal exopolysaccharide PIA - Biosynthesis and role in biofilm formation, colonization, and infection. *Comput Struct Biotechnol J*, 18 (2020) 3324.

26 Kwiecinski JM, Kratofil RM, Parlet CP, Surewaard BGJ, Kubes P & Horswill AR, Staphylococcus aureus uses the ArlRS and MgrA cascade to regulate immune evasion during skin infection. *Cell Rep*, 36 (2021) 109462.

27 Patel H & Rawat S, A genetic regulatory see-saw of biofilm and virulence in MRSA pathogenesis. *Front Microbiol*, 14 (2023) 1204428.

28 Ji N, Yang J & Ji Y, Determining impact of growth phases on capacity of *Staphylococcus aureus* to adhere to and invade host cells. *Methods Mol Biol*, 2069 (2020) 187.

29 Ren Z, Yu J, Du J, Zhang Y, Hamushan M, Jiang F, Zhang F, Wang B, Tang J, Shen H & Han P, A General Map of Transcriptional Expression of Virulence, Metabolism, and Biofilm Formation Adaptive Changes of *Staphylococcus aureus* When Exposed to Different Antimicrobials. *Front Microbiol*, 13 (2022) 825041.

30 Gogoi-Tiwari J, Williams V, Waryah CB, Costantino P, Al-Salami H, Mathavan S, Wells K, Tiwari HK, Hegde N, Isloor S, Al-Sallami H & Mukkur T, Mammary Gland Pathology Subsequent to Acute Infection with Strong versus Weak Biofilm Forming Staphylococcus aureus Bovine Mastitis Isolates: A Pilot Study Using Non-Invasive Mouse Mastitis Model. *PLoS One*, 12 (2017) e0170668.

31 Lacey KA, Gonzalez S, Yeung F, Putzel G, Podkowik M, Pironti A, Shopsin B, Cadwell K & Torres VJ, Microbiome-Independent Effects of Antibiotics in a Murine Model of Nosocomial Infections. *mBio*, 13 (2022) e0124022.

32 Larcombe S, Jiang JH, Hutton ML, Abud HE, Peleg AY & Lyras D, A mouse model of *Staphylococcus aureus* small intestinal infection. *J Med Microbiol*, 69 (2020) 290.

33 Duan L, Zhang J, Chen Z, Gou Q, Xiong Q, Yuan Y, Jing H, Zhu J, Ni L, Zheng Y, Liu Z, Zhang X, Zeng H, Zou Q & Zhao Z, Antibiotic Combined with Epitope-Specific Monoclonal Antibody Cocktail Protects Mice Against Bacteremia and Acute Pneumonia from Methicillin-Resistant *Staphylococcus aureus* Infection. *J Inflamm Res*, 14 (2021) 4267.

34 Kwiecinski JM & Horswill AR, Staphylococcus aureus bloodstream infections: pathogenesis and regulatory mechanisms. *Curr Opin Microbiol*, 53 (2020) 51.

35 Tuffs SW, Goncheva MI, Xu SX, Craig HC, Kasper KJ, Choi J, Flannagan RS, Kerfoot SM, Heinrichs DE & McCormick JK, Superantigens promote Staphylococcus aureus bloodstream infection by eliciting pathogenic interferon-gamma production. *Proc Natl Acad Sci USA*, 119 (2022) e2115987119.

36 Bertram T, Reimers D, Lory NC, Schmidt C, Schmid J, C Heinig L, Bradtke P, Rattay G, Zielinski S, Hellmig M, Bartsch P, Rohde H, Nuñez S, Rosemblatt MV, Bono MR, Gagliani N, Sandrock I, Panzer U, Krebs CF, Meyer-Schwesinger C, Prinz I & Mittrücker HW, Kidney-resident innate-like memory γδ T cells control chronic *Staphylococcus aureus* infection of mice. *Proc Natl Acad Sci USA*, 120 (2023) e2210490120.

37 van den Berg S, Laman JD, Boon L, ten Kate MT, de Knegt GJ, Verdijk RM, Verbrugh HA, Nouwen JL & Bakker-Woudenberg IA, Distinctive cytokines as biomarkers predicting fatal outcome of severe *Staphylococcus aureus* bacteremia in mice. *PLoS One*, 8 (2013) e59107.

38 Dong H, Xiu W, Wan L, Li Q, Zhang Y, Ding M, Shan J, Yang K, Teng Z, Yuwen L & Mou Y, Biofilm microenvironment response nanoplatform synergistically degrades biofilm structure and relieves hypoxia for efficient sonodynamic therapy. *J Chem Eng*, 453 (2023) 139839.

39 Hamamoto H, Panthee S, Paudel A, Ohgi S, Suzuki Y, Makimura K & Sekimizu K, Transcriptome change of *Staphylococcus aureus* in infected mouse liver. *Commun Biol*, 5 (2022) 721.

40 Mohammad M, Na M, Hu Z, Nguyen MT, Kopparapu PK, Jarneborn A, Karlsson A, Ali A, Pullerits R, Götz F & Jin T, Staphylococcus aureus lipoproteins promote abscess formation in mice, shielding bacteria from immune killing. *Commun Biol*, 4 (2021) 432.

41 Thomer L, Schneewind O & Missiakas D, Pathogenesis of Staphylococcus aureus Bloodstream Infections. *Annu Rev Pathol*, 11 (2016) 343.